KINETICS OF GENERATION, RELAXATION, AND ACCUMULATION OF ELECTRONIC EXCITATIONS UNDER TWO-PHOTON INTERBAND PICOSECOND ABSORPTION IN TUNGSTATE AND MOLIBDATE CRYSTALS

V. I. Lukanin, A. Ya. Karasik [*]

Prokhorov General Physics Institute, Russian Academy of Sciences
119991, Moscow, Russia

Under two-photon 523.5 nm interband picosecond laser excitation, we measured the kinetics of induced absorption in $PbWO_4$, $ZnWO_4$, and $PbMoO_4$ crystals with 532 to 633 nm continuous probe radiation. We obtained real-time information about the dynamics of the generation, relaxation, and accumulations of electronic excitations over a wide time range (from picoseconds to hundreds of seconds) and the 77–300 K temperature range. For the studied crystals, exponential temperature-independent growth of the induced absorption (IA) with 60 ns rise time reflects the dynamics of the generation of electronic excitation. The kinetics of the IA exponential growth with temperature-dependent 3.5–$11\mu s$ time constants reflect the dynamics of energy migration between neighboring tungstate (molibdate) ions to traps for the studied crystals. The multiexponential relaxation absorption kinetics strongly depend on temperature, and the relaxation decay time of induced absorption increased from tens to hundreds of ms to seconds under crystal cooling from 300 K to 77 K. We found that the increase in the laser pump repetition rate (0–10 Hz) leads to the accumulation of electronic excitations. Control of the repetition rate and the number of excitations allowed us to change the relaxation time of the induced absorption by more than two orders of magnitude. Due to accumulation of excitations at 77 K, the absorption relaxation time can exceed 100 s for $PbWO_4$ and $PbMoO_4$ crystals. In the initially transparent crystals, two-photon interband absorption (2PA) leads to crystals opacity at the 523 and 633 nm wavelengths. (An inverse optical transmission of the crystals exceeds 50–55 at a 50–100 GW/cm^2 pump intensity.) Measured at ~ 1 mW probe radiation of 532 and 633 nm wavelengths, the induced absorption values are comparable with those obtained under two-photon absorption at ~ 5 kW pump power. An optical 2PA shutter for the visible spectral range is proposed with a variable shutting time from hundreds of microseconds to tens of seconds.

1. INTRODUCTION

Processes concerning the generation and relaxation of electronic excitations in inorganic [1] and organic [2] media are of particular interest. Methods of laser spectroscopy are widely used for investigations of basic properties of materials and interaction of light with matter. In this respect, the nonlinear two-photon absorption (2PA) technique attracts attention due to a number of unique properties. The 2PA technique is applicable to controlling the energy, time, spectral, and spatial parameters of laser radiation [3]. In addition,

the 2PA technique allows increasing the spatial resolution in laser microstructuring of materials and microscopy. The list of 2PA applications can be significantly extended [2].

Two-photon nonlinear spectroscopy can provide new information that is inaccessible by traditional one-photon spectroscopy [4, 5]. The use of the 2PA technique is advantageous, in particular, for excitation of electronic states in the conduction band of materials. For one-photon excitation in a nontransparent spectral range of the conduction band, large nonradiative losses do not allow obtaining bulk homogeneous excitation of a sample [6]. In the case of interband 2PA, the energy of one of the excitation photons can correspond to the transparency region of the material. In this case, selective laser excitation of levels under 2PA can allow di-

[*]E-mail: karasik@lst.gpi.ru

rect examination of luminescence and absorption from the interior of a bulk sample. The difference between the selection rules for one- and two-photon excitation processes provides additional capabilities. The measurement of the 2PA coefficients and cross sections are of independent interest.

The optical properties of oxide tungstate and molibdate crystals are of current interest because of the use of these crystals in scintillation detector of ionizing radiation [1], in addition to their promising use as nonlinear optical materials, e. g., as shifters of a laser radiation frequency via stimulated Raman scattering (SRS) [7, 8]. Applications of the crystals require knowledge of the scintillation response rate. As a rule, this rate is measured using methods of the one-photon florescence spectroscopy. However, a search of new methods for investigations of the dynamics of generation and relaxation of electronic excitations is important. In [9], we demonstrated a method to analyze the dynamics of interband 2PA in tungstate crystals excited by a sequence of picosecond laser pulses of variable intensity while under continuous probe radiation. We measured the 2PA coefficients for several tungstates and molibdates and analyzed the competition between 2PA and SRS [10, 11].

In this paper, we investigate the real-time kinetics of the generation and relaxation of electronic excitations under interband picosecond 2PA and induced absorption (IA) from excited levels in PbWO$_4$ (PWO), PbMoO$_4$ (PMO), and ZnWO$_4$ (ZWO) crystals. The use of 532 to 633 nm continuous probe radiation allows obtaining real-time information about the dynamics of the generation, relaxation, and accumulations of electronic excitations over a wide time range (from picoseconds to hundreds of seconds) and the 77–300 K temperature range. We demonstrate an effect of accumulation of excitations by varying the laser pumping rate and the sample temperature. We show a possibility of an optical shutter creation with a variable shutting time from hundreds of microseconds to tens of seconds.

2. EXPERIMENTAL METHODS AND RESULTS

The experimental setup shown in [10] was modified for this work. The crystals were excited by 523.5 nm trains of transform-limited 20 ps pulses of the second harmonic of a passively mode-locked and Q-switched Nd:YLiF$_4$ laser [12]. The edge of the absorption band varied from 330 nm in (PWO) to 400 nm in (PMO) [10]. The pump photon energy, $h\nu$, corresponds to the transparency region of the crystals and the condition $h\nu < Eg < 2h\nu = 4.74$ eV is satisfied

for the two-photon interband absorption. The linearly polarized single-mode laser 523.5 nm radiation was focused on the 0.5–3 cm long crystal under study to a spot with a beam waist radius of about $26\,\mu m$ by a lens with a focal length of 112 mm. (The Gaussian beam profile of the pump laser radiation was measured with a silicon CCD camera.) Radiation before and after the crystal was directed onto fast Ge or Si photodiodes. The signals were analyzed with a Tektronix DPO 4104 digital oscilloscope with an amplification band of 1 GHz, which determined the time resolution of the recording system. For direct measurement of IA kinetics, ~ 1 mW of a continuous wave (cw) probe, at either 632.8 nm from a He–Ne laser or 532 nm from a frequency doubled Nd laser, was introduced to the crystal collinearly to the picosecond pumping radiation. The output probe radiation after a crystal and diffraction grating was directed to the Si (Ge) photodiode or to a photomultiplier tube (PMT-136) with the resolution time ~ 7 ns. As a rule, an oscilloscope trace was measured in one laser burst. Because of this, we were able to substantially decrease the effect of a geometrical factor on the measurement accuracy as compared to the use of single pulse for the excitation followed by signal accumulation and averaging with many laser bursts.

Figure 1a shows the dependence of the output pulse intensity I on the input pulse intensity I_0 for one of the two orthogonal linear directions of the 523.5 nm excitation polarization with respect to the crystallographic axes of an 18 mm long ZWO crystal. This dependence was obtained by measuring the amplitudes of the corresponding pulses of the train (Fig. 2a) in oscilloscope traces recorded at the input and output of the crystal. Here, the arrow directions indicate a sequential increase or decrease in the pulse intensity when passing from the first to the second half of a train. The essential increase in the input value I_0 was limited by optical breakdown in the crystal. (For the ZWO and PWO crystals, damage was observed at $I_0 > 100$ GW/cm^2, and for PMO, at $I_0 < 10$ GW/cm^2.) Figure 1b shows the ratio of the radiation intensities at the input and output of the crystal, $1/T = I_0/I$, as a function of I_0. Using the linear part of the inverse transmission ($1/T$) dependence in the initial stage, we determined the 2PA coefficients [10, 11]. The 2PA coefficient measured for ZWO is equal to $\beta = 1.1$ cm/GW. (For orthogonal linear directions of the excitation polarization, $\beta = 0.7$ cm/GW.) For PWO and PMO, $\beta = 2.0$–0.8 cm/GW and $\beta = 2.4$–0.9 cm/GW, respectively. The crystals are promising for their use as limiters of laser intensity. Due to 2PA, the output intensity for ZWO is limited at the level ~ 1.85 GW/cm^2
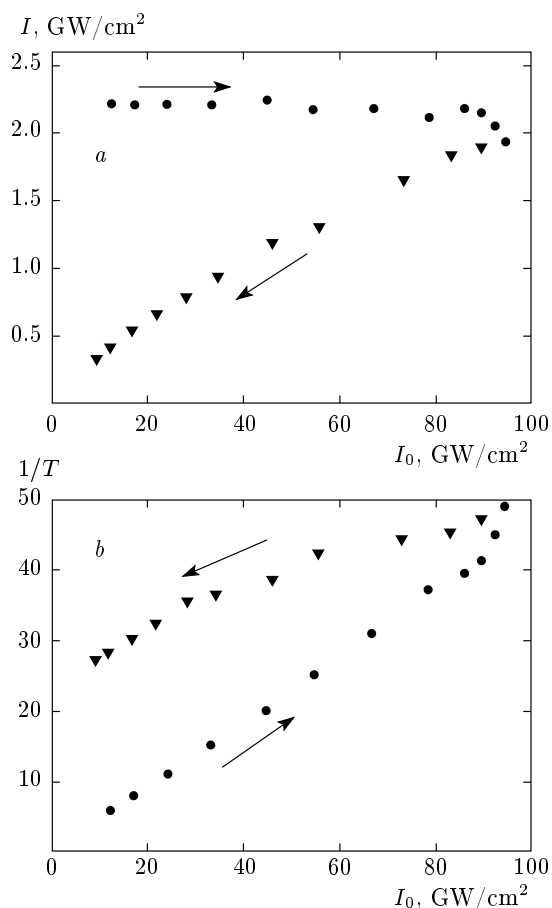
Fig. 1. *a*) Radiation intensity at the output (I) vs. the 532.5 nm excitation intensity at the input (I_0) of an 18 mm long $ZnWoO_4$ crystal, *b*) the inverse transmission $1/T = I_0/I$ vs. I_0 for linear directions of the excitation polarization with respect to the crystallographic axis, $\mathbf{E} \parallel C_2$. The arrows associated with circles indicate the direction of a sequential increase in the intensity I_0 of the excitation pulses in the first half of the train, and the arrows associated with triangles indicate a sequential decrease in the intensity of the excitation pulses in the second half of the train
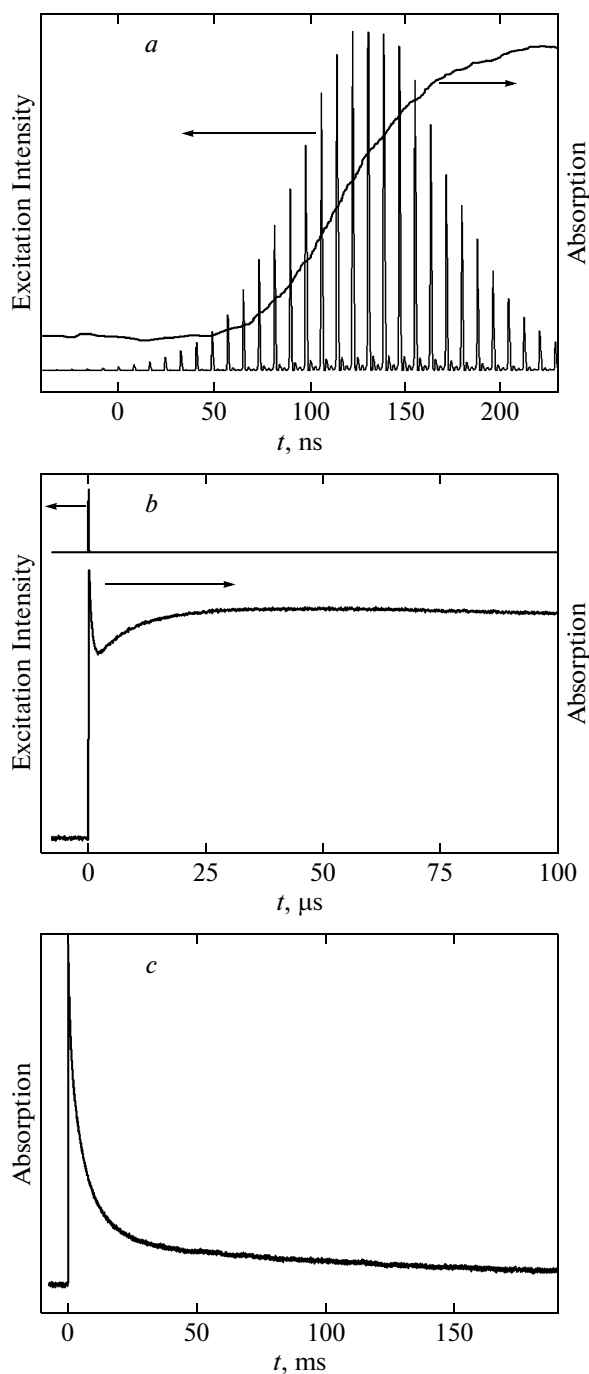

Fig. 2. *a,b*) Oscilloscope trace of a 523.5 nm pumping pulse train and kinetics growth, *c*) relaxation of induced absorption measured at 300 K in a $PbMoO_4$ crystal under $\lambda_{pr} = 532$ nm continuous wave probe radiation

(Fig. 1*a*). (From a calculation, the I_0-independent limiting intensity is $I_{max} = 1/\beta L = 1.9$ GW/cm².) For a 30 mm long PWO and a 6 mm long PMO, the laser pulse intensity is strongly limited due to 2PA at the respective level ~ 2–3 GW/cm² and 0.7–1 GW/cm².

As the intensity of the pump pulses from the second half of the train decreased, the inverse transmission exhibited hysteresis for all crystals. Under 2PA with two 523.5 nm photons, a crystal simultaneously absorbs a third 523.5 nm probe photon from an excited state to another state. Because the excitation time of the latter exceeds the pump train duration of ~ 200 ns, hystere-

sis is seen in Fig. 1. Using picosecond pulsed pumping, we were unable to analyze the kinetics of IA from the excited levels over a wide time range. To accomplish this and investigate the complete dynamics of the excitation and relaxation process, we used continuous wave probe radiation.

Figures 2a and 3a show trains of laser pumping at 523.5 nm. Measured at 300 K, the IA (inverse transmission) kinetics are shown for a probe wavelength of 532 nm in PMO (Fig. 2) and a probe wavelength of 633 nm in PWO (Fig. 3). The kinetics for the probe wavelengths $\lambda_{pr} = 633$ and 532 nm were similar for each crystal. All the kinetics exhibited a fast exponential stage of increase in the absorption with a ~ 60 ns rise time (Figs. 2a and 3a). An absorption decrease stage followed the exponential increase in absorption for PMO (Fig. 2b) and PWO (Fig. 3b). This stage was absent for the ZWO crystal. The time duration of this stage, τ_l, depended on the pumping intensity I_0. For PMO, I_0 was limited to a maximum of ~ 7 GW/cm² by crystal damage and at this intensity, τ_l was ~ 560 ns. For PWO, as I_0 increased from 10 to 100 GW/cm², τ_l increased from 0.6 μs to several μs. After the absorption decrease stage, exponential absorption growth occurred in PMO (Fig. 2b) with the rise time $\tau_{r2} = 8.5$–11.5 μs ($\lambda_{pr} = 532$ nm) and 9–10 μs ($\lambda_{pr} = 633$ nm). For ZWO, the rise time of the corresponding absorption was $\tau_{r2} = 3.5$–4 and 3 μs for the green and red probe wavelengths, respectively. (A scatter in τ_{r2} values for both probe wavelengths occurred due to the linearly polarized excitation of the two optical axes of the crystals.) The absorption rise in this stage for PWO is not pronounced (Fig. 3b). After maximization of the absorption, a multiexponential relaxation was found to occur (Figs. 2c and 3c). The exponential decay constants at the kinetics tail are varied for $\lambda_{pr} = 532$ and 633 nm: 120–180 ms (PMO), 110–230 ms (PWO), and 220–370 ms (ZWO).

We compared the absorption efficiencies of 2PA and IA from the excited state. Because of 2PA in PMO, the measured inverse transmission value $1/T$ was found to be 2.1–2.9 for the excitation intensity $I_0 = 1$ GW/cm² (with the peak pulse power $P = 5.3$ kW). Measured at ~ 1 mW cw probe radiation of 532 and 633 nm wavelengths, the values $1/T \approx 2.0$–2.5 are comparable with those obtained under 2PA at a 5.3 kW power. (We do not give the exact $1/T$ values for the probe wavelengths λ_{pr} because profiles of the pump and probe beams were not ideally matched along the total interaction length.)

The observed IA from excited electronic levels by 2PA is apparently connected with the excitation of crystal defect (trap) levels. Excitation of the energy
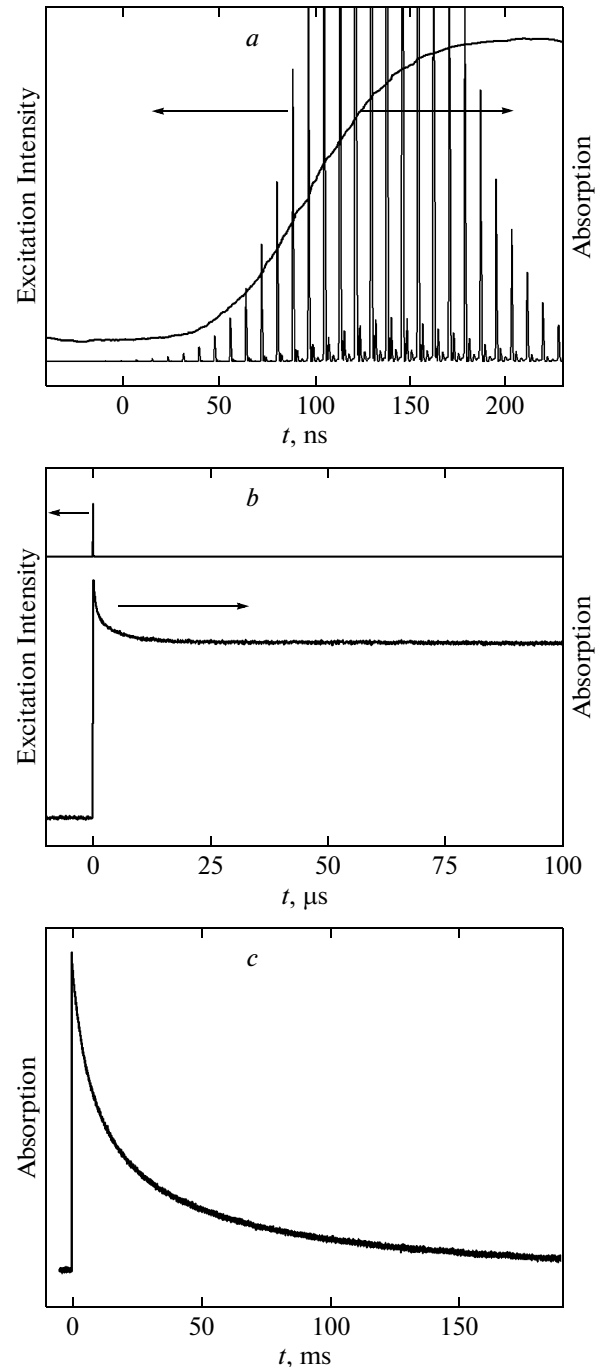

Fig. 3. a, b) Oscilloscope trace of a 523.5 nm pumping pulse train and kinetics growth, c) relaxation of induced absorption measured at 300 K in a $PbWO_4$ crystal under $\lambda_{pr} = 633$ nm continuous wave probe radiation

levels of traps was found in the luminescence study of tungstate and molybdate crystals by one-photon UV excitation [5, 6, 13–16]. It was shown in these works that at low temperatures, a blue (~ 420 nm, PWO) and

green (~ 520 nm, PMO) luminescence corresponded to the excitation of WO_4^{2-} and MoO_4^{2-} molecular ions, while the longer wavelength luminescence (up to red for PMO) was connected with the excitation of the crystals defects. The excitation luminescence spectra for these crystals extended to more than 5 eV [5, 6, 14, 15]. The two-photon 4.74 eV excitation energy in our case leads to the excitation of the WO_4^{2-} and MoO_4^{2-} molecular ions.

A conspicuous IA increase (Figs. 2a and 3a) was found to arise with a 30–50 ns time delay relative to the initial pulses of a train having the intensity $I_0 = 0.05$–5 GW/cm². For this intensity range, 2PA leads to a linear dependence of the inverse transmission on I_0. For $I_0 > 2$–5 GW/cm², IA leads to a departure from the linear $1/T$ dependence and to hysteresis (Fig. 1). But when continuous wave probe radiation is used, we can conclude that after 2PA and excitation of the molecular WO_4^{2-} (MoO_4^{2-}) ion levels, the number of directly excited traps is negligible. The indirect excitation of trap levels is possible due to non-radiative energy migration from the molecular WO_4^{2-} (MoO_4^{2-}) ions. The energy transfer between the molecular WO_4^{2-} ions was studied in [17, 18] for the $CaWO_4$ crystal. In [18], the authors presented a model based on a Frenkel exciton in the WO_4^{2-} complex with a subsequent resonant energy transfer between neighboring tungstate ions to traps. After the two-photon excitation of the ion and its relaxation to the lowest vibrational level of that state by vibrational relaxation on a short time scale (ps or less), energy migration to the traps occurs in the relaxed excited state. We therefore suggest that the kinetics in Figs. 2 and 3 reflect the dynamics of energy migration from excited ions to the traps. The relatively large absorption relaxation times are determined by the radiative and nonradiative relaxation from the trap levels to the ground state.

Figures 4 and 5 show the IA kinetics measured at the crystals cooling from 300 K to 77 K. We note that the characteristic absorption decrease stage at 300 K (Figs. 2b and 3b) is absent at 77 K. Similarly to what was found at 300 K, the IA increase, which is connected to the process of generating electronic excitation, is seen in the fast nanosecond time scale (Figs. 4a and 5a). For all the crystals studied, in the first stage, the induced absorption is exponential with a ~ 60 ns rise time that is independent of the temperature from 77 to 300 K. We note that the front of the envelope of the pumping picosecond pulse train (Figs. 2a and 3a) also increases exponentially. We suggest that the rate of generation of electronic excitations is related to the time derivative of the picosecond pump train envelope.
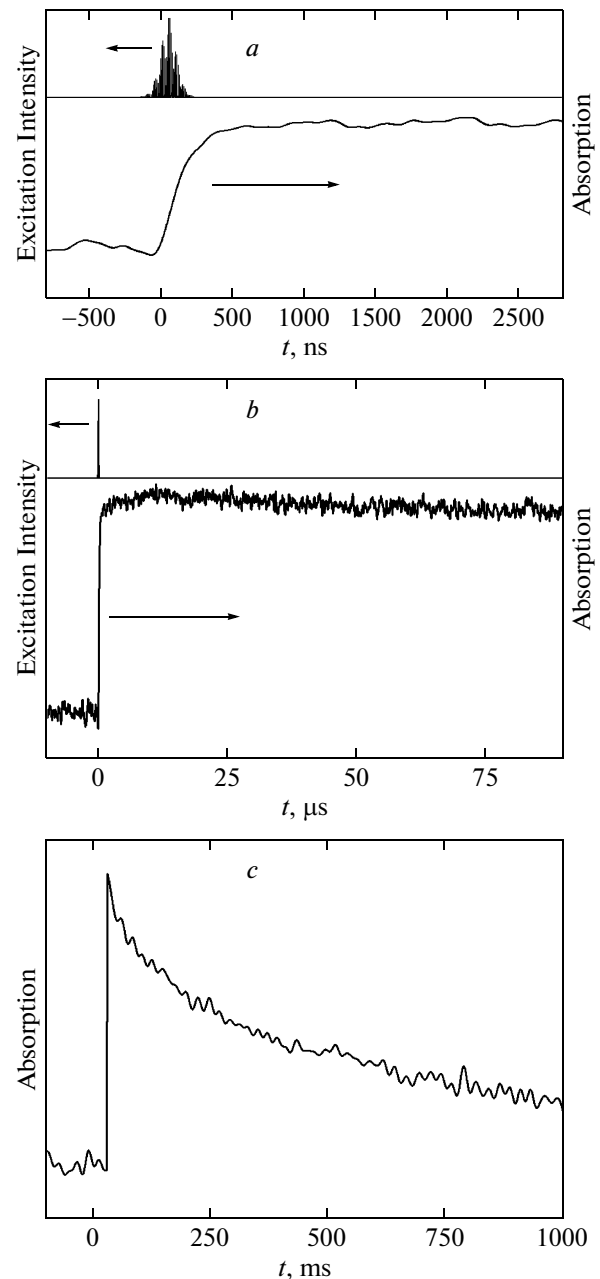

Fig. 4. a, b) Oscilloscope trace of a 523.5 nm pumping pulse train and kinetics growth, c) relaxation of induced absorption measured at 77 K in a $PbMoO_4$ crystal under $\lambda_{pr} = 633$ nm continuous wave probe radiation

The kinetics of the IA increase in the microsecond time range (Figs. 4b and 5b at 77 K and Figs. 2b and 3b at 300 K) correspond to the process of energy migration between neighboring tungstate (molibdate) ions to traps. The crystal cooling from 300 K to 77 K leads to an approximately two-fold decrease in the IA rise time, to 3.6 μs for PMO and to 7.1 μs for PWO. We
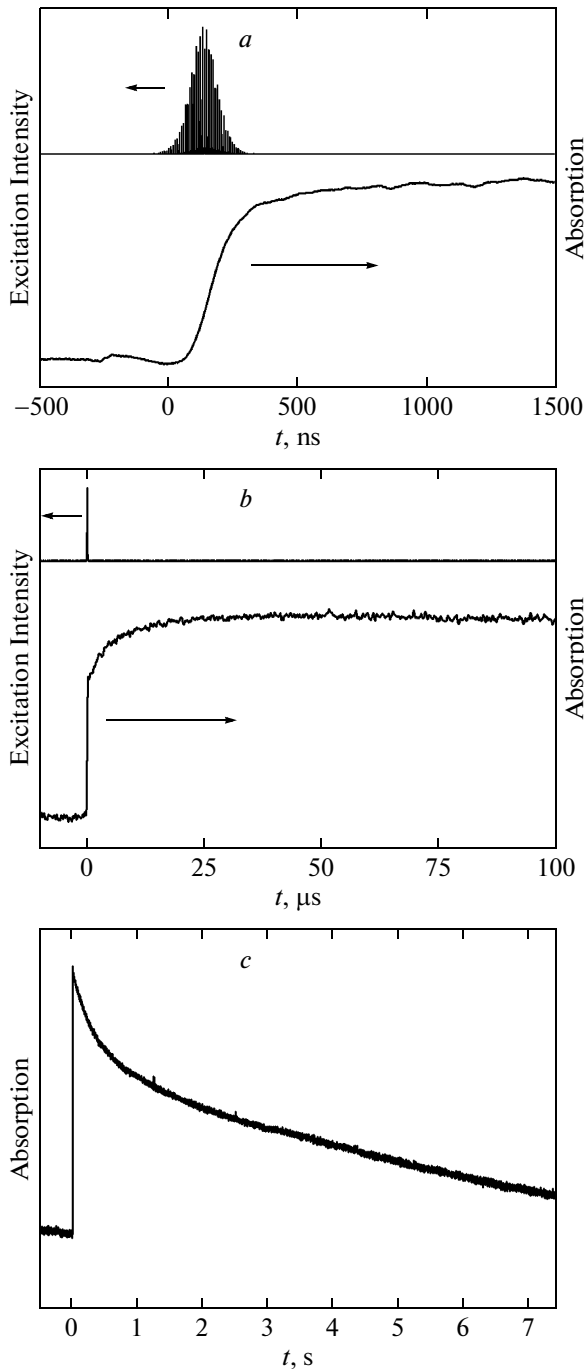
Fig. 5. a, b) Oscilloscope trace of a 523.5 nm pumping pulse train and kinetics growth, c) relaxation of induced absorption measured at 77 K in a $PbWO_4$ crystal under $\lambda_{pr} = 633$ nm continuous wave probe radiation

note that treating the excitation migration as a diffusion process, the authors of [18] showed that the rate of energy transfer to the traps approaches a constant value above 100 K. Under crystal cooling from 300 K to
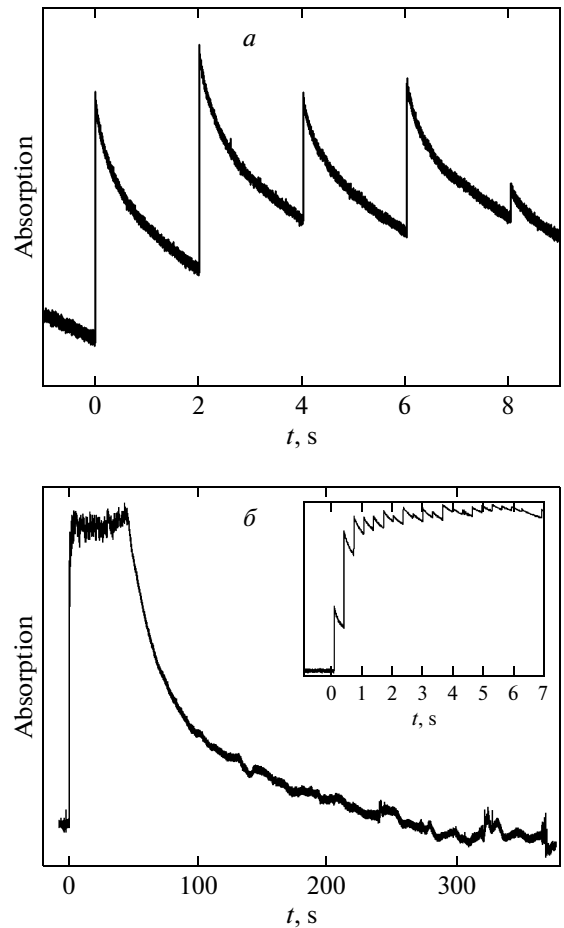

Fig. 6. a) Kinetics of induced absorption in the crystal $PbWO_4$ measured at a 0.5 Hz laser pumping with the repetition rate 523.5 nm (77 K, $\lambda_{pr} = 633$ nm), b) kinetics of induced absorption in the crystal $PbWO_4$ measured at 77 K after repeated laser pumping at 3 Hz and excitation accumulation. The kinetics at the induced absorption increase stage is shown in the inset on an expanded time scale

77 K, an essential change in the absorption relaxation kinetics is observed (Figs. $4c$ and $5c$), with the decay time of IA being increased many times, from tens to hundreds of ms to seconds. A significant increase in the IA relaxation time is obviously caused by population of the low trap levels.

An increase in the pumping repetition rate leads to the accumulation of excitations, which becomes apparent at 77 K for a 0.5 Hz rate (PWO) (Fig. $6a$). After one of the laser pumping pulses, the IA relaxation to the ground state is incomplete upon arrival of the next pumping pulse. This leads to a subsequent increase in IA. After several excitations at 3 Hz, the IA reaches

a practically constant level (Fig. 6*b*). Upon shutting off the excitation, IA relaxation occurs with the decay time $\tau_{rel} \approx 140$ s for the kinetic tail (for PMO in the same conditions, $\tau_{rel} \approx 100$ s). Hence, control of the pumping repetition rate and the number of pumping pulses allows changing the IA relaxation time by more than two orders of magnitude. Taking into account that the inverse optical transmission of the crystals exceeds 50–55 at the pump intensity ~ 50–100 GW/cm^2 and the crystals at 2PA became opaque in the visible (523, 633 nm) spectral range, an optical shutter is obtained with a variable shutting time over a wide temporal range.

A possibility of a creation of the population inversion under 2PA attracts the attention for further investigations. Creation of lasers with two-quantum transitions was proposed for the first time by Prokhorov (Nobel Prize lecture, 1964) [19]. In the studied crystals, after 2PA and fast multiphonon relaxation to the excited relaxed state, the population inversion could arise. Along with 2PA, the process of two-step interband absorption with tunable picosecond laser excitation can facilitate the creation of population inversion. After two-step absorption with first one-photon resonant excitation, fast excitation relaxation to a relatively long-lived metastable level should occur. We note that we observed an intense blue luminescence in the studied ZWO, PWO, and PMO crystals excited by 2PA at 300 K and 77 K. The above effect of accumulation of the excitations should contribute to the creation of the population inversion.

3. CONCLUSION

Using the 2PA technique, we investigated the dynamics of the generation and relaxation of electronic excitations in tungstates and molibdates crystals. The sequence of 523.5 nm picosecond laser pulses of variable intensity was used for the 2PA excitation, and we measured the kinetics of the induced absorption from excited levels of molecular WO_4^{2-} (MoO_4^{2-}) ions of the crystals with 530 and 633 nm continuous wave probe radiation. We elucidated that a single exponential increase in the induced absorption that is independent of temperature in the range from 300 to 77 K and has a 60 ns time constant reflects the process of the generation of electronic excitations in the crystals. We suggest that the kinetics of the generation of electronic excitation are related to the time derivative of the picosecond pump train envelope. The kinetics of IA exponential growth with temperature-dependent 3.5–11 μs time

constants for the studied crystals reflect the dynamics of energy migration between neighboring tungstate (molibdate) ions to traps. The multiexponential relaxation absorption kinetics strongly depend on temperature, and the relaxation decay time of IA increases from tens to hundreds of milliseconds to seconds under crystal cooling from 300 to 77 K. We found that the increase in the pumping repetition rate leads to the accumulation of electronic excitations. Control of the repetition rate and the number of excitations allow changing the IA relaxation time by more than two orders of magnitude. At 77 K, the absorption relaxation time can exceed 100 s for $PbWO_4$ and $PbMoO_4$ crystals.

The values of the induced absorption in a PMO crystal measured at ~ 1 mW continuous wave probe radiation of 532 and 633 nm wavelengths are comparable to those obtained under 2PA at 5.3 kW power. Taking into account that 2PA leads to crystals opacity at the 523, 633 nm wavelengths, an optical 2PA shutter for the visible spectral range is proposed with a variable shutting time from hundreds of microseconds to tens of seconds.

REFERENCES

1. M. Nikl, Phys. Stat. Sol. (a) **178**, 595 (2000).

2. M. Rumi and J. W. Perry, Adv. Opt. Phot. **2**, 451 (2010).

3. V. V. Arsenyev, V. S. Dneprovskii, D. N. Klyshko, and A. N. Penin, JETP **29**, 413 (1969).

4. W. Kaiser and C. G. B. Garret, Phys. Rev. Lett. **7**, 229 (1961).

5. V. B. Mikhailik, H. Kraus, D. Wahl et al., Phys. Rev. B **69**, 205110 (2004).

6. J. A. Groenik and G. Blasse, J. Sol. St. Chem. **32**, 9 (1980).

7. T. T. Basiev, P. G. Zverev, A. Ya. Karasik et al., JETP **99**, 934 (2004).

8. P. Becker, L. Bohaty, H. J. Eichler, H. Rhee, and A. A. Kaminskii, Laser Phys. Lett. **4**, 884 (2007).

9. V. I. Lukanin, D. S. Chunaev, and A. Ya. Karasik, JETP Lett. **91**, 548 (2010).

10. V. I. Lukanin, D. S. Chunaev, and A. Ya. Karasik, JETP **113**, 412 (2011).

11. V. I. Lukanin, D. S. Chunaev, and A. Ya. Karasik, Frontiers in Optics, Laser Science XXVII FIO/LS Technical Digest, paper LTuE4 (2011).

12. A. Ya. Karasik and D. S. Chunaev, JETP Lett. **85**, 315 (2007).

13. M. Nikl, K. Nitsch, K. Polak et al., Phys. Stat. Sol. (b) **195**, 311 (1996).

14. W. van Loo, Phys. Stat. Sol. (a) **27**, 565 (1975).

15. G. Tamulaitis, S. Buracas, V. P. Martinov et al., Phys. Stat. Sol. (a) **157**, 187 (1996).

16. A. Annenkov, E. Auffray, M. Korzhik, P. Lecoq, and J.-P. Peigneux, Phys. Stat. Sol. (a) **170**, 47 (1998).

17. D. L. Dexter and J. H. Schulman, J. Chem. Phys. **22**, 1063 (1954).

18. M. J. Treadaway and R. C. Powell, J. Chem. Phys. **61**, 4003 (1974).

19. A. M. Prokhorov, Sov. Phys. Usp. **85**, 599 (1965).